Fifis, T., & Scopes, R. K. (1978) *Biochem. J. 175*, 311–319.
Jaffe, E. K., Nick, J., & Cohn, M. (1982) *J. Biol. Chem. 257*, 7650–7656.
Leyh, T. S., Sammons, R. D., Frey, P. A., & Reed, G. H. (1982) *J. Biol. Chem. 257*, 15047–15053.
Macara, I. G. (1980) *Trends Biochem. Sci. (Pers. Ed.) 5*, 92–94.
Mildvan, A. S., & Cohn, M. (1970) *Adv. Enzymol. Relat. Areas Mol. Biol. 33*, 1–70.
Murmann, R. K. (1976) *Inorg. Chem. 16*, 46–51.
Nageswara Rao, B. D., Cohn, M., & Scopes, R. K. (1978) *J. Biol. Chem. 253*, 8056–8060.
Norris, J. R., Uphaus, R. A., Crespi, H. L., & Katz, J. J. (1971) *Proc. Natl. Acad. Sci. U.S.A. 68*, 625–628.
Pecoraro, V. L., Hermes, J. D., & Cleland, W. W. (1984) *Biochemistry 23*, 5262–5271.
Pickover, C. A., McKay, D. B., Engelman, D. M., & Steitz, T. A. (1979) *J. Biol. Chem. 254*, 11323–11329.
Reed, G. H., & Leyh, T. S. (1980) *Biochemistry 19*, 5472–5480.
Reed, G. H., & Markham, G. D. (1984) *Biol. Magn. Reson. 6*, 73–142.
Roustan, C., Fattoum, A., Jeanneau, R., & Pratel, L. (1980) *Biochemistry 19*, 5168–5175.
Scopes, R. K. (1971) *Biochem. J. 122*, 89–92.
Scopes, R. K. (1973) *Enzymes (3rd Ed.) 8*, 335–351.
Simons, T. J. B. (1979) *Nature (London) 281*, 337–338.
Tanswell, P., Westhead, E. W., & Williams, R. J. P. (1976) *Eur. J. Biochem. 63*, 249–262.
Tsai, M. (1979) *Biochemistry 18*, 1468–1472.
Watson, H. C., Walker, N. P. C., Shaw, P. J., Bryant, T. N., Wendell, P. L., Fothergill, L. A., Perkins, R. E., Conroy, S. C., Dobson, M. J., Tuite, M. F., Kingsman, A. J., & Kingsman, S. M. (1982) *EMBO J. 1*, 1635–1640.
Webb, M. R., Ash, D. E., Leyh, T. S., Trentham, D. R., & Reed, G. H. (1982) *J. Biol. Chem. 257*, 3068–3072.

Comparison of the Active Sites of Atropinesterase and Some Serine Proteases by Spin-Labeling

A. C. M. van der Drift,* G. W. H. Moes,‡ E. van der Drift,§ and B. A. C. Rousseeuw§
Medical Biological Laboratory TNO, 2280 AA Rijswijk, The Netherlands
Received March 12, 1985

ABSTRACT: The side chain of the serine residue in the active center of atropinesterase (AtrE), α-chymotrypsin (Chymo), and subtilisin A (Sub) was labeled with two paramagnetic reporter groups of different size (label I or II, respectively) by sulfonylation with *N*-[3-(fluorosulfonyl)phenyl]-1-oxy-2,2,5,5-tetramethylpyrroline-3-carboxamide or *N*-[6-(fluorosulfonyl)-2-naphthyl]-1-oxy-2,2,5,5-tetramethylpyrroline-3-carboxamide. ESR spectra of labeled enzymes in 10 mM phosphate buffer, pH 7.4, were measured at temperatures between 133 and 298 K by using a home-built spectrometer operating in the absorption mode at 10-kHz field modulation. The spectra, in particular those at 276–298 K, were analyzed by computer simulation of the overall line shape according to the methods developed by Freed and co-workers, based on eigenfunction expansion. In the case of AtrE for both labels, the best agreement between experimental and simulated solution spectra was obtained with only one mobility component showing anisotropic, axially symmetric reorientation according to the Egelstaff jump–diffusion model. The axis of preferential reorientation was found to lie in the XZ plane at a polar angle of about 30° with the X axis. The corresponding rotational correlation time ($\tau_{\parallel}$) did not show appreciable viscosity/temperature (η/T) dependence but had a constant value of 4.4 and 2.2 ns for labels I and II, respectively. The rotational correlation time associated with rotation around the axes perpendicular to that of preferential reorientation ($\tau_{\perp}$) showed the usual η/T dependence and had a value of 22.0 ns at 276 K for both labels. The above results strongly suggest that in AtrE both nonpolar reporter groups reside in a pocket near the active serine. Contrary to the situation in AtrE, the overall mobility of the –N–O· fragments in Chymo and Sub was found to result from contributions of at least two distinct motional states, strongly and weakly immobilized. In going from label I to label II, the relative contribution of the latter state increases at the expense of that of the former. This is ascribed to an equilibrium between a relatively free state of the aromatic cores and a firmly bound position in the specificity pocket of these proteases. The apparently more rigid embedding of the spin-labels in the enzyme structure of AtrE suggests that the size of the nonpolar binding pocket in the active center region of this esterase allows a deeper penetration of the aromatic portions of the labels than is possible for the specificity pocket of Chymo or Sub.

Stable nitroxide radicals [cf. Rozantsev (1970)] have been widely applied as spin-labels in enzymology (Berliner, 1974, 1978; Morrisett, 1976) and in biomedical research (Chignell, 1979; Piette & Hsia, 1979) because they have proven to be useful reporter groups for probing the structure of specific sites in a biomolecular environment. Their ESR[1] spectra reflect both the effect of interactions between label and biomolecule

‡Present address: Prins Maurits Laboratory TNO, 2280 AA Rijswijk, The Netherlands.
§Present address: Department of Applied Physics, University of Technology, Delft, The Netherlands.

[1] Abbreviations: AtrE, atropinesterase; Chymo, α-chymotrypsin; Sub, subtilisin A; DFP, diisopropyl phosphorofluoridate; ESR, electron spin resonance.

0006-2960/85/0424-5333$01.50/0

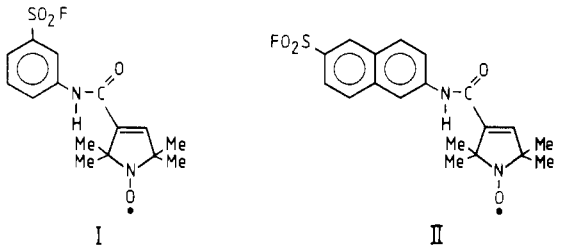

FIGURE 1: Molecular structures of *N*-[3-(fluorosulfonyl)phenyl]-1-oxy-2,2,5,5-tetramethylpyrroline-3-carboxamide (label I) and *N*-[6-(fluorosulfonyl)-2-naphthyl]-1-oxy-2,2,5,5-tetramethylpyrroline-3-carboxamide (label II).

on the mobility of the –N–O· fragment and the polarity of the direct environment (Berliner, 1974, 1978; Griffith et al., 1974; Jost & Griffith, 1978). This information may supplement the results obtained by other methods such as X-ray diffraction, NMR, and fluorescence spectrometry.

Serine proteases may be irreversibly inhibited by different alkyl and aromatic sulfonyl fluorides by sulfonylation of their active serine (Fahrney & Gold, 1963; Sigler et al., 1966; Wright et al., 1969). With spin-labeled benzenesulfonyl fluorides, analogues of the inhibitor tosyl fluoride, structurally different nitroxide spin-labels may be specifically attached to the active serines of both α-chymotrypsin and trypsin (Berliner & Wong, 1974; Wong et al., 1974). This approach allows a more detailed comparison of the spatial structure of the environment of this amino acid residue in different enzymes than the usual one with only one spin-label.

Atropinesterase from *Pseudomonas putida* strain L of the biotype A (strain PMBL-1)[2] is a serine esterase that specifically catalyzes the hydrolysis of (–)-atropine to (–)-tropic acid and tropine (Berends et al., 1967; Stevens, 1969; Rörsch et al., 1971; Hessing, 1983). Within the scope of the physicochemical characterization of this enzyme by means of various techniques (Van der Drift, 1983), the environment of its active serine (at position 110) has been compared with that of the well-known serine proteases α-chymotrypsin and subtilisin A by using nitroxide spin-labels of different size as reporter groups. All three enzymes are irreversibly inhibited by spin-labeled benzenesulfonyl fluoride (I) and spin-labeled naphthalenesulfonyl fluoride (II) (Figure 1) by specific sulfonylation of the side chain of the active serine. Label I was used to allow comparison with other investigations (Berliner & Wong, 1974) whereas label II was suggested by fluorescence investigations on these enzymes labeled with a dansyl group (Van der Drift, 1983). Contrary to related work on chymotrypsin and trypsin (Berliner & Wong, 1974), detailed spectrum simulation by using the rigorous theory for slowly tumbling spin-labels (Freed et al., 1971; Freed, 1972, 1976) has been attempted for the interpretation of the experimental ESR spectra. This quantitative approach allows a more detailed characterization of the active site region of these enzymes than the qualitative methods used by Hoff et al. (1971).

Materials and Methods

Enzymes. Salt-free α-chymotrypsin (M_r 24 800; EC 3.4.21.1) from bovine pancreas (3 × crystallized and lyophilized) was purchased from Sigma Chemical Co. (lot C-4129). Dialyzed and lyophilized subtilisin A (M_r 27 300; EC 3.4.21.14) was obtained from NOVO Industri A/S (batches 73-1, A 8003-75, and A 9001-75). Atropinesterase (M_r 30 300) was isolated from *Pseudomonas putida* PMBL-1 and purified according to the procedure of Rörsch et al. (1971) as modified by Oosterbaan et al. (personal communication). For α-chymotrypsin and subtilisin A the amounts of active enzyme in the preparations used were found to be about 75% and 60%, respectively [cf. Van der Drift (1983)]. Atropinesterase was almost pure as shown by polyacrylamide gel electrophoresis (one band) and isoelectric focusing (one main band and a few minor bands) [cf. Hessing (1983)]. Enzyme activities were determined by acidimetric titration according to the pH-stat method described elsewhere (Van der Drift, 1983) with *N*-acetyl-L-tyrosine ethyl ester (Merck) as a substrate for α-chymotrypsin and subtilisin A and with (–)-atropine sulfate (Nutritional Biochemicals Corp.) for atropinesterase. Total enzyme concentrations were determined spectrophotometrically at 280 nm with $E_{280}^{0.1\%}$ = 2.04, 0.96, and 1.85 for α-chymotrypsin (Chymo), subtilisin A (Sub), and atropinesterase (AtrE), respectively [cf. Van der Drift (1983)].

Nitroxide Spin-Labels. The fluorosulfonyl radicals *N*-[3-(fluorosulfonyl)phenyl]-1-oxy-2,2,5,5-tetramethylpyrroline-3-carboxamide and *N*-[6-(fluorosulfonyl)-2-naphthyl]-1-oxy-2,2,5,5-tetramethylpyrroline-3-carboxamide (Figure 1) were synthesized as described in the Appendix. For the inhibition, 10 mM solutions in dry acetone were used. These solutions were kept at 277 K in the dark. All commercially available chemicals used were reagent grade, unless stated otherwise.

Preparation of Spin-Labeled Enzymes. To 1.0 mL of an enzyme solution (about 0.1 mM in 10 mM sodium phosphate buffer, pH 7.4, containing 0.1 mM sodium azide to prevent growth of bacteria) 35 μL of a solution of radical I or II was added. The mixture was incubated at room temperature in the dark for 12–16 h, until inhibition was complete (residual enzyme activity less than 1% of the original activity). Since the solubility of the radicals, in particular of label II, in water was very limited (≤0.3 mM) some precipitate of excess radical was always present during incubation. After inhibition this precipitate was removed by centrifugation. Subsequently, the protein solution was dialyzed for 48–72 h at 277 K in the dark against frequently renewed 150 mL of phosphate buffer. Increase in enzyme activity during dialysis was negligible. In order to check homogeneity, solutions of labeled enzymes were routinely subjected to gel filtration at 277 K on a Sephadex superfine G-50 column. All enzymes were eluted as a single peak as measured by absorbance at 280 nm. Spectroscopically, no difference was observed between the various fractions of the protein peak. Protein solutions were kept in the dark and investigated by ESR as soon as possible after completion of the dialysis in order to minimize contamination by any release of spin-label (see below). To improve the signal to noise ratio, in some cases solutions were concentrated at 277 K by means of Minicon Macrosolute concentrators, type A 25 (Amicon). Protein solutions were 0.05–0.2 mM.

ESR Spectrometry. Electron spin resonance measurements of the enzyme preparations were taken at X-band (9 GHz) on a home-built spectrometer (Mehlkopf, 1970; Mehlkopf et al., 1972) operating in the absorption mode at 10-kHz field modulation. The microwave field was kept below the level of observable saturation. Similarly, the amplitude of the field modulation was small compared with the line widths in order to prevent spectrum distortion. Samples were contained in thin Pyrex glass capillaries (1 mm inner diameter) centered along the symmetry axis of the cylindrical TE 011 cavity. Measurements were done at various temperatures (±0.5 K) in the range 133–298 K.

[2] This notation refers to the culture collection of the Medical Biological Laboratory TNO.

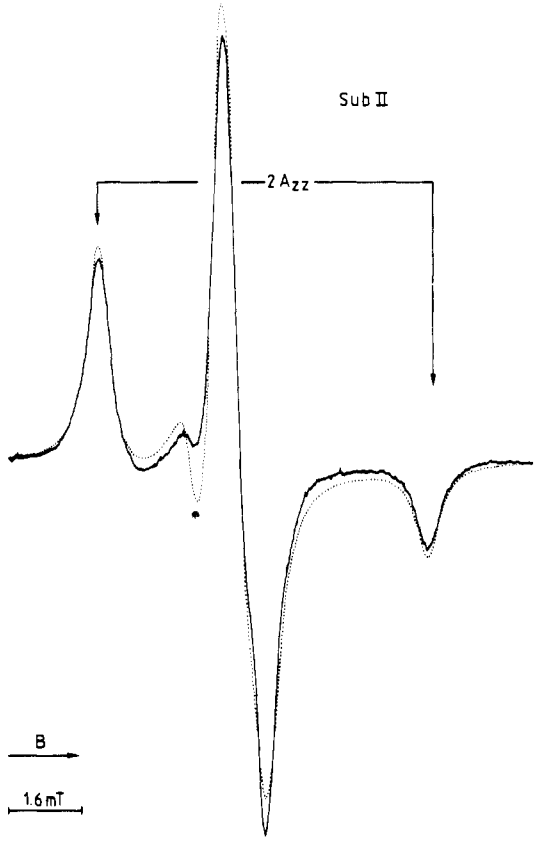

FIGURE 2: Comparison between the experimental rigid limit spectrum of label II bound to subtilisin (Sub) at 213 K (—) and the corresponding simulated spectrum (···). The value of $2A_{zz}$ equals the distance between the outer extrema. Best agreement was obtained with $\alpha = 0.3$ mT and $\beta = 0.05$ mT for the angle-dependent residual line width.

Table I: Principal Values of the Zeeman Interaction Tensor ($\bar{\bar{g}}$) and the Nuclear Hyperfine Coupling Tensor ($\bar{\bar{A}}$) Used in the Present Analysis

tensor	X axis	Y axis	Z axis
$\bar{\bar{g}}^a$	2.0088	2.0062	2.0027
$\bar{\bar{A}}$ (mT)^b	0.623	0.623	3.596

[a] Obtained from Libertini & Griffith (1970). [b] Obtained from rigid limit and solution spectra.

Spectral Analysis. Spectral analysis was achieved by computer simulation of the overall line shape according to the methods developed by Freed and co-workers (Freed et al., 1971; Freed, 1972, 1976), on the basis of eigenfunction expansion. For that purpose, the principal values of the nuclear hyperfine coupling tensor ($\bar{\bar{A}}$) and the Zeeman interaction tensor ($\bar{\bar{g}}$), which in principle can be obtained from an analysis of the rigid limit spectra, have to be known. For labels I and II, these values are not available in the literature, whereas the resolution in the center of the rigid limit spectra is too small to allow an accurate direct determination of the X and Y components of these tensors. An example of the rigid limit spectra of the labeled enzymes at low temperatures is given in Figure 2. In the present analysis, the accurate principal values of $\bar{\bar{g}}$ determined for di-*tert*-butyl nitroxide (DTBN; Libertini & Griffith, 1970) were used for both spin-labels (Table I). In single-host crystals, spectra of DTBN were reported to be very similar to those of 2,2,5,5-tetramethyl-3-oxopyrrolidine-1-oxyl (Griffith et al., 1965), which in turn are considered to be very similar to those of the pyrrolinyl spin-labels. It is assumed that in solution the similarity between

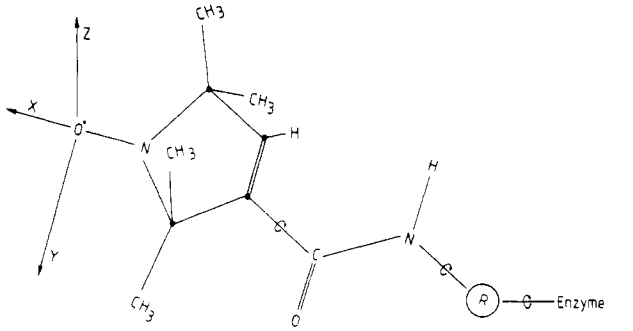

FIGURE 3: Molecular reference frame as defined for nitroxide radicals and the rotations around bonds in the side chain connecting the –N–O· fragment with the enzyme. R = sulfonylated aromatic moiety. The molecular Z axis is perpendicular to the pyrrolinyl ring.

DBTN and the pyrrolinyl spin-labels is unaltered.

The value of A_{zz} was obtained directly from the distance between the extrema at low and high magnetic field in the rigid limit spectrum (Figure 2). Since in free nitroxide radicals $\bar{\bar{A}}$ is found to be almost axially symmetric around the Z axis, the values of A_{xx} and A_{yy} were assumed to be equal and were obtained from the isotropic hyperfine splitting $a_{iso} = (A_{xx} + A_{yy} + A_{zz})/3 = 1.614$ mT, observed in buffer, and the value of A_{zz}. These principal values of $\bar{\bar{A}}$ are also listed in Table I. Within experimental accuracy, no differences were found between the two labels bound to the three enzymes. For free nitroxide radicals, the principal axes of $\bar{\bar{A}}$ and $\bar{\bar{g}}$ can be assumed to coincide (Libertini & Griffith, 1970).

In order to verify the above assumptions, the experimental spectrum in Figure 2 has been reconstructed via the program of Polnaszek (1976) by using the values of Table I. This simulation required an angle-dependent residual line width $\alpha + \beta \cos^2 \theta$, where θ is the polar angle between the external magnetic field and the principal Z axes of $\bar{\bar{A}}$ and $\bar{\bar{g}}$ and α and β are constants to be assessed. The best agreement between experimental and simulated spectrum was obtained with $\alpha = 0.3$ mT and $\beta = 0.05$ mT. Figure 2 shows that agreement is satisfactory.

Variables related to the reorientation of the –N–O· fragment that remain to be assessed via spectrum simulation are principal values of the rotational diffusion tensor $\bar{\bar{R}}$ (or of the corresponding correlation times τ), including the position of its principal axes in the molecular frame, the reorientation model, e.g., Brownian, free or jump diffusion, and the rotationally invariant line width [cf. Bruno (1973), Freed (1976), and Polnaszek (1976)]. Unless stated otherwise, the latter parameter could be set to zero. Figure 3 shows the molecular reference frame as usually defined for nitroxide radicals and to which the components of $\bar{\bar{A}}$ and $\bar{\bar{g}}$ are related (Smith, 1972).

The computer program used for slowly tumbling simulations (Polnaszek, 1982) was a more rapid and corrected version of that given elsewhere (Polnaszek, 1976) and is confined to axially symmetric rotational diffusion with the option of noncoinciding Z axes for $\bar{\bar{R}}$ and for $\bar{\bar{A}}$ and $\bar{\bar{g}}$.

Results

ESR spectra of the labeled enzymes at 276 and 298 K are shown in Figures 4 and 5, respectively. When the enzymes were inhibited with diisopropyl phosphorofluoridate (DFP), i.e., when a diisopropyl phosphoryl group was covalently attached to the active serine [cf. Baker (1975)], before treatment with spin-label no ESR signal was observed. In view of this and investigations on specific sulfonylation of serine hydrolases (Fahrney & Gold, 1963; Gold & Fahrney, 1964; Gold, 1965; Cardinaud & Baker, 1970), it may be assumed that after

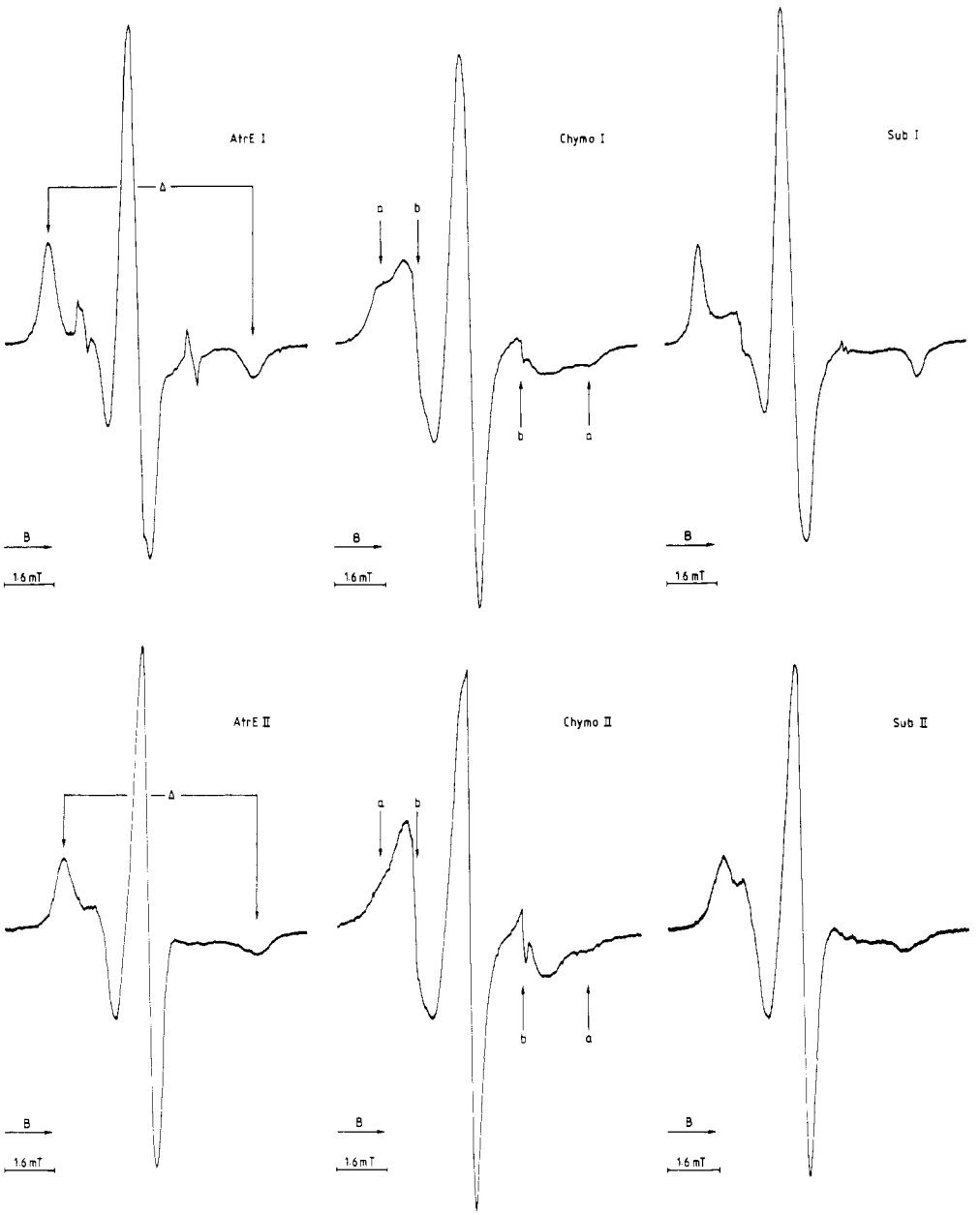

FIGURE 4: Experimental spectra of atropinesterase (AtrE), α-chymotrypsin (Chymo), and subtilisin A (Sub) with labels I (upper row) and II at 276 K in 10 mM phosphate buffer, pH 7.4. Δ = distance between the outer extrema. Outer extrema of the slow and more rapid motional components discernible in the spectra of Chymo are indicated by (a) and (b), respectively. The very sharp satellite lines on either side of the central line are due to unbound label.

treatment with spin-label the enzyme molecule contains just one spin probe bound to the active serine.

The spectra with label I invariably revealed the presence of unbound label. The concentration of this rapidly reorienting component showed a gradual increase with time and temperature and was reduced temporarily by dialysis at 277 K. This phenomenon was also reported by other investigators and can be ascribed to either hydrolytic desulfonylation of the reporter group from the enzyme (Fahrney & Gold, 1963; Gold, 1965) or to intramolecular hydrolysis of the label (Wong et al., 1974). By measuring the ESR spectra as soon as possible after dialysis at 277 K, contamination was kept small: for AtrE maximally 1% of the overall ESR absorption and for the other enzymes somewhat more. Label II was found to be released to a lesser extent at all temperatures.

In general, the spectra of AtrE, Chymo, and Sub at 276 K (Figure 4) and 298 K (Figure 5) clearly showed a distance Δ between the extrema at low and high magnetic field that exceeded the value of $2a_{iso}$ = 3.23 mT appreciably (Table II). This points to the presence of labeled enzyme molecules with the mobility of the –N–O· fragment in the slow motional region. In addition, most spectra of Chymo (Figures 4 and 5) suggested the presence of at least one more rapidly reorienting component with $\Delta \simeq 2a_{iso}$. For Sub, the spectral indications for such a mixture of mobility components were

Table II: Distance (±SE, mT) between Outer Extrema in Solution Spectra of Various Serine Hydrolases with Labels I and II at 276 and 298 K

	label I		label II	
	276 K	298 K	276 K	298 K
atropinesterase	6.52 ± 0.04	6.20 ± 0.04	6.16 ± 0.08	5.68 ± 0.12
α-chymotrypsin	6.60 ± 0.12	6.36 ± 0.32	6.60 ± 0.32	*a*
subtilisin	6.92 ± 0.04	6.68 ± 0.04	5.72 ± 0.06	5.33 ± 0.16

[a] Slow motional component not discernible.

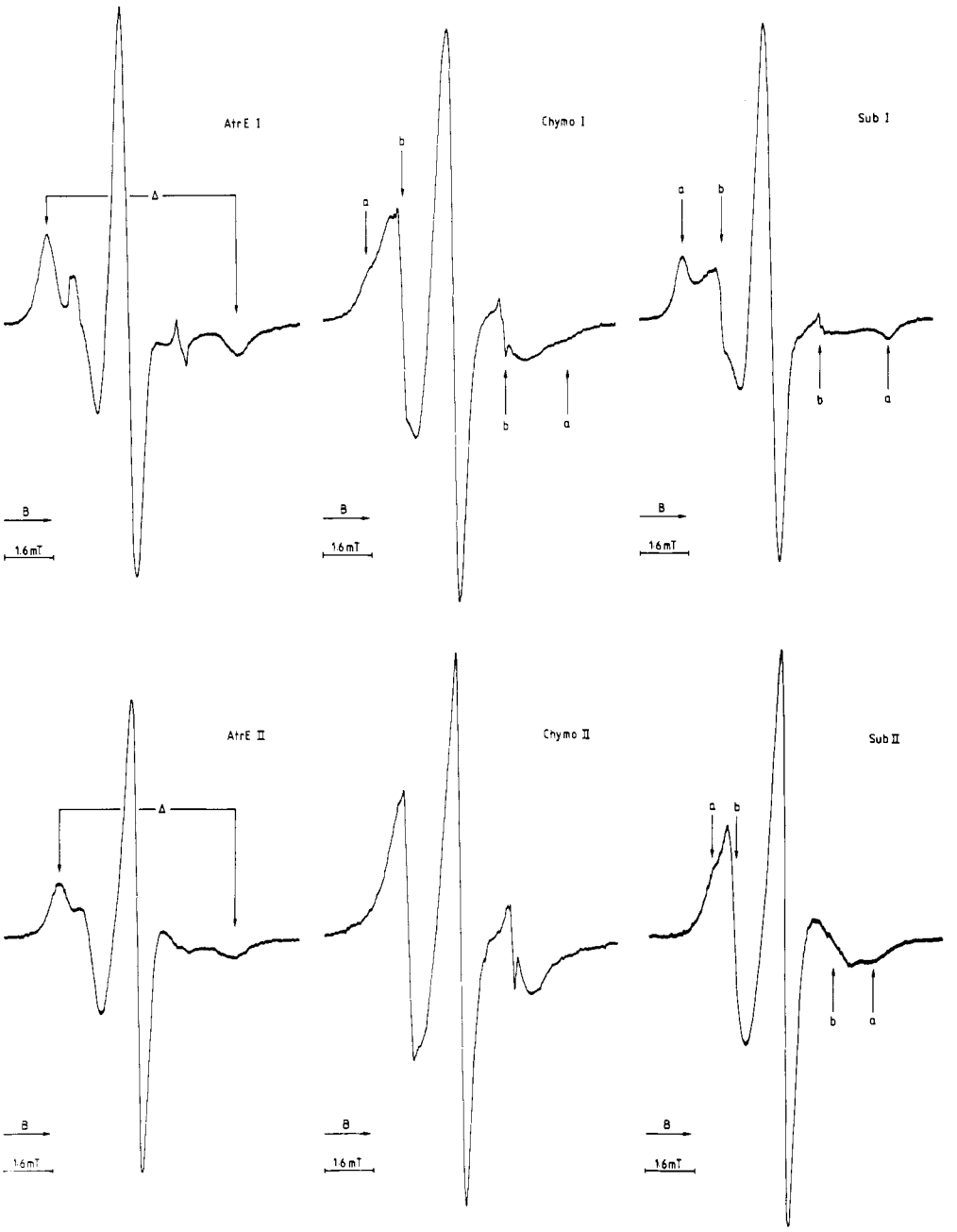

FIGURE 5: Experimental spectra of atropinesterase (AtrE), α-chymotrypsin (Chymo), and subtilisin A (Sub) with labels I (upper row) and II at 298 K in 10 mM phosphate buffer, pH 7.4. Δ = distance between the outer extrema. Outer extrema of the slow and more rapid components discernible in the spectra of Chymo and Sub are indicated by (a) and (b), respectively. The very sharp satellite lines on either side of the central line are due to unbound label.

hardly observable at 276 K (Figure 4) but obvious at 298 K (Figure 5). The spectra of AtrE are attributable to only one mobility component. For the latter enzyme, as for the slow motional species of Sub, the value of Δ for label I is larger than that for label II (Table II), which indicates that the –N–O· fragments have a different mobility under similar conditions. For Chymo, such a difference was not observed at 276 K (Table II). These qualitative characteristics of the experimental solution spectra in terms of one or more components with a characteristic mobility have been analyzed in more detail by spectrum simulation.

Reconstruction of the Spectra of Atropinesterase. Detailed reconstruction of the slow motional spectra of labeled AtrE was started by assuming reorientation of a single mobility component by isotropic Brownian rotational diffusion. Simulations of the experimental spectra at 276 K (Figure 6A,B) were obtained by adjusting the rotational correlation time τ_R to approximate the line positions as close as possible. The best values of τ_R were 15.0 and 6.7 ns for label I and label II, respectively.

The experimental spectra at 298 K were simulated with τ_R = 7.9 ns for label I and τ_R = 3.5 ns for label II (Figure 6C,D). These values were calculated from those at 276 K by imposing the usual viscosity/temperature (η/T) dependence for isotropic rotational diffusion.

For both labels, but in particular for label II, the simulated overall line shapes in Figure 6 deviate substantially from those of the experimental spectra. Nevertheless, some conclusions relevant for further analysis can be drawn: (1) As it may be assumed that the essential features of the reorientation process are the same for label I and label II, the significantly smaller Δ of label II at 276 K (Table II) is a strong indication that the –N–O· fragment of this larger label has a definite motional freedom relative to the enzyme moiety. This is supported by

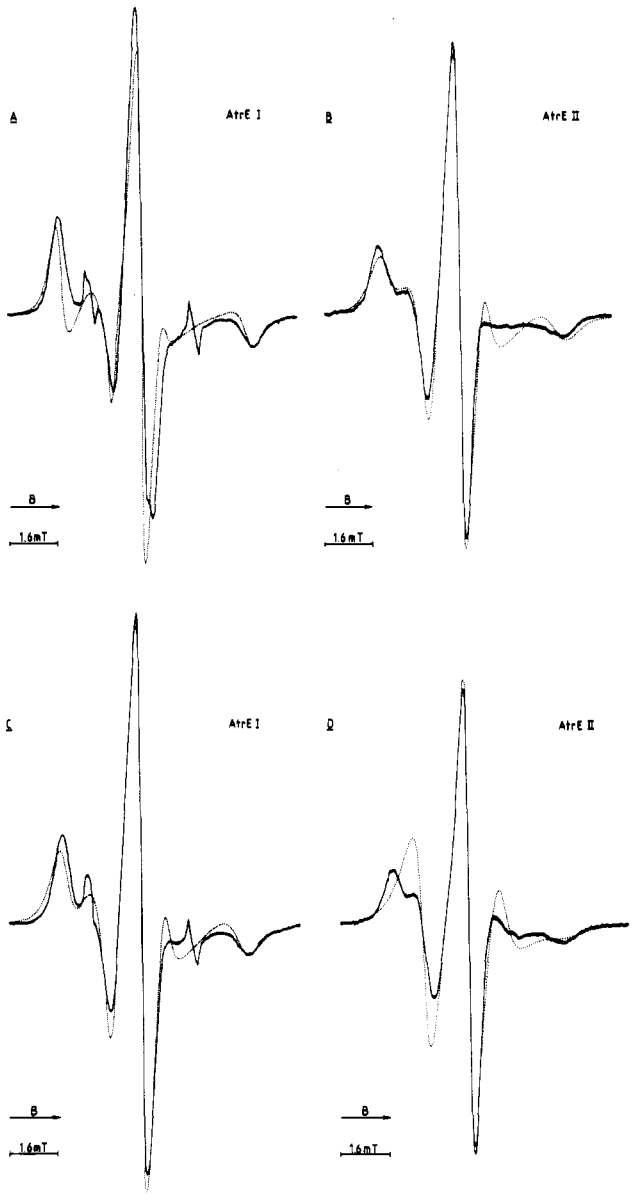

FIGURE 6: Comparison of the experimental solution spectra (—) and corresponding optimized computer simulations (···) for atropinesterase (AtrE) with labels I and II at 276 (A and B) and 298 K (C and D). Simulations are based on the isotropic Brownian rotational diffusion model. Best values of τ_R at 276 and 298 K: for label I, 15.0 and 7.9 ns, respectively; for label II, 6.7 and 3.5 ns, respectively.

the comparison of the best value of τ_R of label II with the theoretical lower limits of 16 and 32 ns, respectively, estimated on the basis of the Stokes–Einstein relation [cf. Carrington & McLachlan 1967)] for an anhydrous monomer or dimer [cf. Van der Drift (1983)] at this temperature. (2) In contrast to label I, extension of the simulations to 298 K for label II leads to a substantially smaller Δ than experimentally observed (Figure 6D). This points to contributions to the orientation of the –N–O· fragment that are not hydrodynamically (η/T) controlled.

These conclusions suggest that the mobility of the –N–O· fragment in label II results from reorientation of the enzyme in solution and from rotations around bonds in the side chain connecting the ESR-sensitive group to the enzyme [cf. Buchachenko & Wasserman (1982)]. Although for label I the evidence of such a composite mobility is less pronounced, the similarity of the molecular structures of both labels (Figure 1) justifies the assumption that this more general mobility concept applies to this label as well. Any difference between

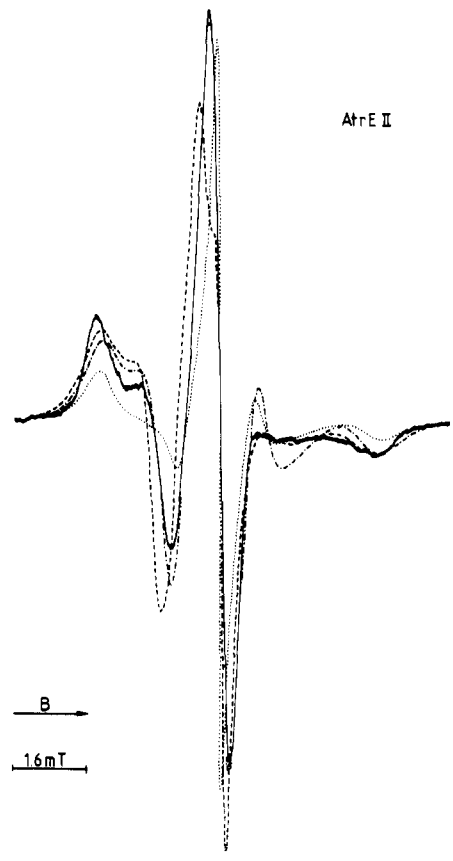

FIGURE 7: Comparison between the experimental (—) and simulated spectrum for atropinesterase (AtrE) with label II at 276 K. Simulations were performed on the basis of anisotropic reorientation (anisotropy factor = 10) according to axially symmetric Brownian rotational diffusion with preferential reorientation around the molecular X (– –), Y (···), and Z axes (–·–).

comparable spectra of label I and II can then be ascribed to the effect of a different aromatic core on the rotational mobility of the side chain. The significantly larger size of label II over label I makes it likely that possible differences in this mobility will result from different interactions with the protein rather than from differing internal mobilities of the labels per se. Because of the anisotropic nature of the rotations in the side chain (Figure 3), some anisotropy may be anticipated for the composite motion of the –N–O· fragment.

A rough test for the validity of the anisotropic model is shown in Figure 7, where simulations for AtrE with label II at 276 K are given, on the basis of axially symmetric Brownian rotational diffusion. In this model the anisotropic mobility is described by two rotational diffusion coefficients, $R_\parallel$ and $R_\perp$, with $R_\parallel$ accounting for preferential reorientation (i.e., $R_\parallel > R_\perp$) around some axis and $R_\perp$ for reorientation around axes perpendicular to this symmetry axis. The corresponding rotational correlation times are defined as $\tau_\parallel = 1/(6R_\parallel)$ and $\tau_\perp = 1/(6R_\perp)$. In Figure 7, simulations with the axis of preferential reorientation collinear with the molecular X, Y, or Z axis (Figure 3) are compared. The anisotropy factor $N = R_\parallel/R_\perp$ was chosen to be 10, and the individual values of $R_\parallel$ and $R_\perp$ were adjusted to approximate the experimental line positions as close as possible. Obviously, preferential reorientation around the molecular Y axis ($\tau_\parallel$ = 3.75 ns) leads to less agreement with the experimental spectrum than that around the X ($\tau_\parallel$ = 3.0 ns) or Z axis ($\tau_\parallel$ = 0.6 ns). Preferential reorientation around an axis collinear with the –N–O· bond (X axis: Figure 3) leads to the best reconstruction because in this case the difference between the measured and the

Table III: Values of Rotational Correlation Times of Atropinesterase with Labels I and II at Different Temperatures As Obtained from Optimized Simulations according to the Anisotropic Jump–Diffusion Model[a]

correlation time (ns)[b]	label I		label II	
	276 K	298 K	276 K	298 K
$\tau_\parallel$	4.4	4.4	2.2	2.2
$\tau_\perp$	22.0	11.6	22.0	11.6

[a] For details, see text. [b] $\tau_\parallel$ = correlation time of preferential rotation around the symmetry axis; $\tau_\perp$ = correlation time of rotation around axes perpendicular to the symmetry axis. Estimated error is 10%.

simulated absorption next to the high-field side of the central line is minimal, whereas the other parts of the spectrum remain in fair agreement with the experimental line shape. Physically, this outcome is not unreasonable in view of the internal rotational modes of the side chain (Figure 3), the contributions of which to $R_\parallel$ will be larger than those to $R_\perp$. In further refinement of the simulations, this result has to be taken into account.

In view of the numerous degrees of motional freedom in the composite reorientation of the –N–O· fragments and the limited possibilities to account for this properly in the available theories for label reorientation in the slow motional region, the ultimate reconstructions of the spectra at different temperatures were inevitably approximative and were based on assumptions inferred from the above results: (1) The superposition of two types of motion governing reorientation, i.e., the continuous process of Brownian rotational diffusion of the enzyme and the jump-like character of the rotations around bonds in the side chain, was approximated by a single jump–rotational diffusion process accounting for deviations from the Brownian limit of infinitesimally small jumps [Egelstaff jump–diffusion model; cf. Bruno (1973) and Polnaszek (1976)]. (2) The anisotropic reorientation process was assumed to be axially symmetric, i.e., describable by diffusion coefficients $R_\parallel$ and $R_\perp$. (3) In view of the physical principles underlying the anisotropic reorientation process, $R_\perp$ will be mainly determined by the tumbling of the enzyme, i.e., governed by η/T. The preferential reorientation, $R_\parallel$, will be mainly determined by the more rapid rotations in the side chain, negligibly dependent on η/T but rather on the enzyme structure.

The final reconstructions of the spectra of AtrE under these assumptions yield the results in Figure 8. For 276 K, the various parameters were adjusted until the best agreement with the experimental overall line shape was obtained. For both labels the axis of preferential reorientation ($R_\parallel$) was found to lie in the molecular XZ plane at a polar angle of about 30° with the X axis. The correlation times $\tau_\parallel$ and $\tau_\perp$ corresponding with the best $R_\parallel$ and $R_\perp$, respectively, are compiled in Table III. $\tau_\parallel$ is larger for label I and for label II whereas $\tau_\perp$ is the same for both. The deviation from the Brownian model of infinitesimally small jumps results in a mean jump angle of about 12°.

Reconstructions at 298 K were performed similarly by applying the third assumption above. Since there are no indications for an appreciable conformational change of the active site region upon increasing the temperature from 276 to 298 K (Van der Drift, 1983), the polar angle and the mean jump angle were taken equal to those at 276 K. Restricted variation of $R_\parallel$, $R_\perp$, and the polar angle did not improve the results but rather worsened the agreement.

The insensitiveness of $\tau_\parallel$ to temperature variation suggests a rather small (≤1 kcal/mol) activation energy for the rotations in the side chains. From a physical point of view, however, such a low value is rather unlikely, and a rotational activation energy of at least 3–4 kcal/mol is expected, implying a substantial temperature dependence of $\tau_\parallel$ (Owen, 1974; Buchachenko et al., 1980; Bullock 1980). The result emphasizes the complexity of the actual motion and points to counteractive contributions resulting from small temperature-dependent changes in the local structure of the enzyme near the label. These motional effects are neglected in the above analysis since they cannot be dealt with properly at present. Notwithstanding the inevitably approximative character of the present approach and the obvious imperfections in the agreement between reconstructed and experimental spectra in Figure 8 the anisotropic reorientation model with a different temperature dependence for $R_\parallel$ and $R_\perp$ is a substantial improvement in comparison with the isotropic model (Figure 6), particularly for label II. This is stressed even more by $\tau_\perp$ = 22 ns at 276 K for both labels, which is in the range of the theoretical lower limits of 16 and 32 ns for AtrE as either an anhydrous monomer or dimer. This value is smaller than the overall correlation time of 37 ns estimated in a rather

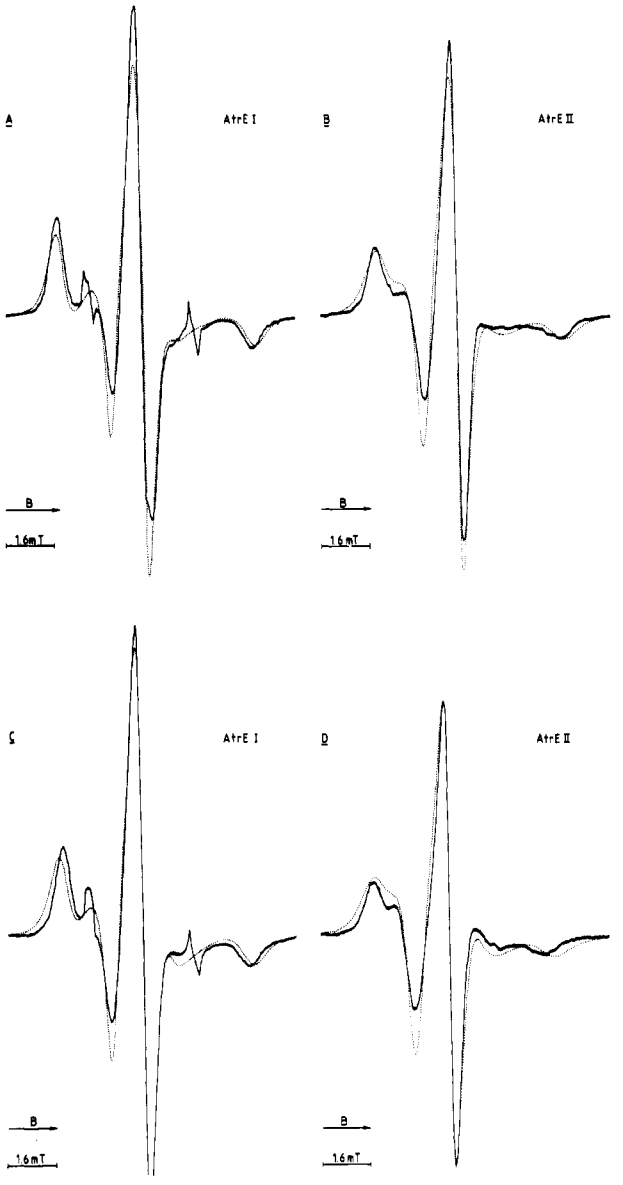

FIGURE 8: Comparison between experimental solution spectra (—) and optimized simulations (···) for atropinesterase (AtrE) with labels I and II at 276 (A and B) and 298 K (C and D). Simulations are based on the anisotropic jump–diffusion model as described in the text.

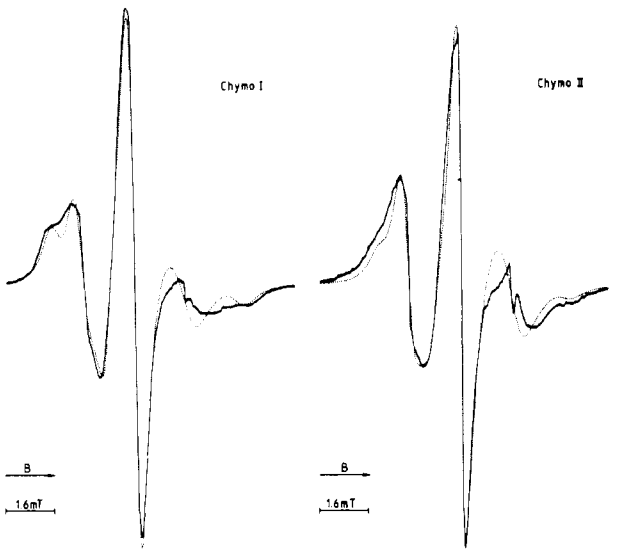

FIGURE 9: Comparison of the experimental solution spectra (—) and corresponding simulations (···) for α-chymotrypsin (Chymo) with labels I and II at 276 K. Simulations are based on the presence of a mixture of two mobility components, the ratio of which is different for Chymo I and Chymo II, respectively (see text).

qualitative way for AtrE inhibited with 1-oxy-2,2,6,6-tetramethyl-4-piperidinyl methylphosphonofluoridate, assuming isotropic reorientation (Hoff et al., 1971).

Reconstruction of the Spectra of α-Chymotrypsin and Subtilisin A. A similar mobility analysis of the spectra of Chymo and Sub is practically impossible because the important regions on both sides of the central line, at a distance of about 1.3 mT, are largely obscured by overlap with the spectra resulting from other mobility components. However, less detailed line-shape simulations are feasible that are consistent with the presence of a mixture of components with different mobilities. This is illustrated in Figure 9, which shows simulations for Chymo on the basis of Brownian rotational diffusion for a mixture of two components. With an agreement comparable to that obtained for AtrE, it was possible to simulate the spectra of both labels with the same two mobility components in different proportions. The best reconstructions were obtained with anisotropic reorientation of the –N–O· fragment with preferential reorientation around the molecular X axis for the slowest component ($\tau_\parallel$ = 4 ns; $\tau_\perp$ = 40 ns; rotationally independent line width 0.05 mT) and around the molecular Y axis for the more rapidly reorienting component ($\tau_\parallel$ = 0.75 ns; $\tau_\perp$ = 7.5 ns; rotationally independent line width 0.15 mT). The fraction of the slowest component was about 0.55 for label I and 0.30 for label II. In view of the uncertainties about the number of mobility components and the type of reorientation process, these simulations can only serve as a demonstration of the principle of superposition. No physical meaning should be attributed to the characteristics of the single components.

The spectra of Sub at higher temperatures (Figure 5), which clearly indicate the presence of different mobility components, can also be analyzed with Brownian rotational diffusion of two single-mobility components showing anisotropic reorientation of the –N–O· fragment. From a limited number of simulations in the case of Sub with label I at 298 K, the fraction of the slower component was about 0.8. For Sub with label II this fraction was estimated at 0.3 because of the great similarity of this spectrum with that of Chymo with label II at 276 K. In contrast to the situation in Chymo, the mobility of the slower component of label I bound to Sub was different from that of label II as can be concluded from the different value of Δ (Table II). In this respect, Sub resembles AtrE more than Chymo.

Discussion

The results obtained by reconstructions according to the above model of anisotropic motion, e.g., the values of $\tau_\parallel$ and $\tau_\perp$ at different temperatures (Table III), strongly suggest that in AtrE at least the nonpolar aromatic portions of the spin-labels are situated in a pocket-like structure near the active serine. The values of $\tau_\parallel$ indicate that the –N–O· fragment of label II has more degrees of freedom for rotations around bonds in the side chain and thus a higher mobility than that of the smaller label I; so, most likely, it protrudes farther outside the protein structure.

Evidence for a pocket-like structure capable of binding a nonpolar group near the active serine in AtrE was also obtained from fluorescence data on a dansyl group bound to the active serine (Van der Drift, 1983). Also the large downfield shift of the ^{31}P resonance observed by NMR upon ageing of AtrE phosphorylated with diisopropyl phosphorofluoridate points to a crevice-like structure close to the active serine in which the remaining isopropyl group is bound (Van der Drift, 1983). In this respect, AtrE resembles Chymo and Sub for which X-ray diffraction studies revealed a so-called primary substrate specificity pocket at the acyl group side, adjacent to the active serine, which preferentially binds the nonpolar side chain of the amino acid residue preceding the hydrolyzable bond of the substrate [cf. Blow (1974) and Kraut (1977)].

As only one spin-label is present per enzyme molecule bound to the active serine, the occurrence of at least one rather mobile (weakly immobilized) motional state for the –N–O· fragment in Chymo and Sub in addition to a strongly immobilized one indicates that the mobility of the probe in these proteases is subjected to an equilibrium between different conformational states. Data obtained by others with Chymo and trypsin (Berliner & Wong, 1974) also indicated that there may be several interconvertible modes of immobilizing a spin-label at the active serine. The strongly immobilized state appears to be favored when the size of the aromatic portion of the side chain is smaller. Therefore, it may reflect a kind of incorporation of the side chain into a crevice-like structure near the active serine as found for AtrE.

Apparently, the embedding of the spin-labels in the protein structure is much less rigid in Chymo and Sub than in AtrE as more rapidly reorienting components do not occur in the latter. This points to a deeper penetration of the aromatic portions of the labels into the structure of AtrE than into that of the proteases. A better fit in the AtrE structure is consistent with results of a comparative fluorescence study of these enzymes, which show that a dansyl group bound to the active serine is much more exposed to solvent in Chymo and Sub than in AtrE (Van der Drift, 1983).

The equality of Δ for the strongly immobilized component of the labels when bound to Chymo (Table II) points to a more or less complete immobilization of the aromatic parts of the side chains. For the slowest component of Sub, the results in Table II indicate that the naphthyl core of label II is appreciably less tightly bound to the enzyme than the phenyl core of label I. An intermediate situation exists for the strongly immobilized state of AtrE since, according to Table II, the naphthyl core is more mobile than the phenyl core but to a less extent than for Sub.

The above-mentioned differences between Chymo and Sub can be related to a different structure of the primary substrate specificity pocket. In Chymo, this hydrophobic binding site is a geometrically well-defined slit-shaped pocket, consisting

of two planar and parallel sides between which only planar, preferentially aromatic groups of particular size and shape can be sandwiched; for Sub, it is a less well-defined shallow crevice being planar only on one side and irregular on the other, which, therefore, imposes less stringent geometrical requirements on size and shape of the interacting group (Kraut et al., 1971; Robertus et al., 1972; Blow, 1974). For the strongly immobilized fractions of Chymo and Sub with label I or II, the plane aromatic portion of the side chain will, at least partly, be wedged in the binding pocket. In Chymo this interaction will leave at most a few degrees of freedom and thus lead to a rather complete immobilization of that section of the side chain for both labels. On the other hand, the geometry of the pocket in Sub will allow the naphthyl group somewhat more motional freedom than the smaller phenyl core.

The better fit in the AtrE structure may be ascribed to larger dimensions of its binding pocket, e.g., a greater depth and/or width. In AtrE, the pocket is presumably deeper than that in Sub in view of the shallow nature of the primary substrate binding site in the latter. The less complete immobilization of the naphthyl core as compared with the phenyl core indicates that, similar to the situation in Sub, the width of the binding pocket in AtrE may be larger than that of the slit-shaped pocket in Chymo.

According to the above point of view, the occurrence of strongly and weakly immobilized fractions for Chymo and Sub labeled with I or II may be traced back to an equilibrium between free and specifically bound aromatic cores at the substrate specificity pocket. The increase in the strongly immobilized fraction of label I and several other labels in Chymo upon addition of indole at pH 3.5 observed by Berliner & Wong (1974) might therefore point to an increased binding of the aromatic core in the specificity pocket rather than to a displacement of the label to another even stronger binding site at the protein surface near the active serine as suggested by these authors (Berliner & Wong, 1974).

The indications of a pocket-like binding site in AtrE near the active serine, in combination with those for an oxyanion hole and a so-called charge-relay system (Van der Drift, 1983), point to a close structural resemblance between the active-site region of this esterase and the active centers of the proteases belonging to the prothrombin-related and the subtilisin superfamilies, which are known to contain these characteristic elements essential to catalysis [cf. Kraut (1977)]. This indicates a mechanism of catalysis by AtrE similar to that by these proteases. It is therefore expected that the tropic acid moiety in the substrate (−)-atropine will require a specific binding site in AtrE during the acylation step of the hydrolysis of the ester bond. In view of the bulky size of this group and its nonpolar character, the presence of a large hydrophobic binding pocket adjacent to the active serine in AtrE can thus be understood.

ACKNOWLEDGMENTS

We thank Dr. R. A. Oosterbaan and F. J. A. Kouwenberg for the isolation and purification of atropinesterase and Ir. J. F. Bleichrodt and Prof. Dr. Ir. J. Smidt for their critical reading of the manuscript.

APPENDIX

Syntheses of Spin-Labels. (*A*) *N-[3-(Fluorosulfonyl)-phenyl]-1-oxy-2,2,5,5-tetramethylpyrroline-3-carboxamide* (*Label I*). Synthesis of this meta compound was partly based on the procedure of Wong et al. (1974) for the ortho analogue. A total of 1.84 g (10 mmol) of 3-carboxy-2,2,5,5-tetramethylpyrroline-1-oxyl, prepared according to Rozantsev (1970), was dissolved in a mixture of 30 mL of benzene and 2 mL of pyridine. Dropwise addition of excess thionyl chloride (1 mL) at room temperature resulted in a deep yellow solution and a white precipitate of pyridine hydrochloride. After being stirred for about 30 min at 20 °C, 2.43 g (13.9 mmol) of *m*-aminobenzenesulfonyl fluoride, prepared by treating *m*-aminobenzenesulfonyl fluoride hydrochloride salt (Aldrich) in tetrahydrofuran with excess pyridine, in 20 mL of benzene was added. Another 2 mL of pyridine was added in order to maintain a basic reaction mixture.

After this was stirred for 1 h, 200 mL of water was added, which resulted in a three-phase system of benzene, water, and a precipitate. The latter was collected by filtration, washed with water, dried, and redissolved in acetone. The solution was filtered and evaporated to dryness in vacuo. The residue was recrystallized from acetone/water, and the solid material was stirred with 20 mL of boiling toluene. After being cooled to room temperature, the solid material was collected by filtration. This extraction procedure was repeated 4 times. The yield of the yellowish product was 2.08 g (60%), mp 218–219 °C. Thin-layer chromatography (TLC) was carried out on Merck Silicagel F 254 Fertigplatten with a mixture of ethyl acetate and methylene chloride (50/50 v/v) as the mobile phase. One spot (R_f 0.70) was detected by fluorescence (excitation at 254 and 360 nm) and iodination. No product was found in benzene or water. Characteristic infrared wavenumbers (cm^{-1}) were 3370 (–NH), 1672 (C=O), 1424, 1404, and 1205 (SO_2), 778 (SF), and 750 and 690 (meta substitution). The mass spectrum (M = 341) was in accordance with the molecular structure of label I.

The above method differs from that of Wong et al. (1974) in that thionyl chloride is used [cf. Krinitskaya et al. (1966)] instead of isobutyl chloroformate. This modification yielded appreciably better results. Moreover, chromatographic purification of the spin-label can be omitted since pure products are obtained.

(*B*) *N-[6-(Fluorosulfonyl)-2-naphthyl]-1-oxy-2,2,5,5-tetramethylpyrroline-3-carboxamide* (*Label II*). Synthesis of label II was analogous to that of label I except that the *m*-aminobenzenesulfonyl fluoride solution was replaced by 2.25 g (10 mmol) of 2-aminonaphthalene-6-sulfonyl fluoride (see below) in 20 mL of acetone/benzene (50/50 v/v). After being stirred for 1 h, the mixture was shaken with 400 mL of a saturated sodium bicarbonate solution, and the yellow precipitate was collected by filtration and washed with water and benzene. Purification of the product was similar to that of label I by recrystallization from water/acetone and repeated extraction with toluene. The yield was 1.87 g (46%), mp 233 °C. TLC was carried out as with label I, R_f 0.70. No impurities were found. Characteristic infrared wavenumbers (cm^{-1}) were 3385 (NH), 1677, 1533, and 1288 (amide), and 1400 and 1193 (SO_2). The mass spectrum (M = 391) was in accordance with the molecular structure of label II.

2-Aminonaphthalene-6-sulfonyl fluoride was prepared [cf. British patent (1956)] by slowly adding 10 mL (173 mmol) of fluorosulfuric acid (Aldrich) to 7.7 g (34 mmol) of 2-aminonaphthalenesulfonic acid (technical grade, Pfaltz and Bauer). With continuous stirring, the mixture was heated to 140–150 °C, allowed to cool slowly to room temperature, and then poured onto 200 mL of crushed ice. After melting of the ice, the white precipitate was collected by filtration. A second batch of product was obtained by neutralization of the filtrate with solid sodium bicarbonate and filtration of the precipitate. The combined fractions were thoroughly washed on a glass filter with 200 mL of a saturated sodium bicarbonate solution

(3 ×) and 50 mL of water (3 ×) and, finally, recrystallized from acetone/water and dried in a vacuum desiccator. The yield of the white product was 2.43 g (33%), mp 148–148.5 °C. Anal. Calcd for $C_{10}H_8FNO_2S$ (M = 225.25): C, 53.22; H, 3.58; F, 8.44; N, 6.22; S, 14.24. Found: C, 53.33–53.38; H, 3.47–3.52; F, 8.42–8.45; N, 6.19–6.25; S, 14.23–14.24. TLC as described above showed one spot, R_f 0.50, with fluorescence detection (excitation at 254 and 360 nm). Characteristic infrared wavenumbers (cm^{-1}) were 3475 and 3375 (NH_2), 1632 (NH_2 + aromatic), 1399 (SO_2 asymmetric + NH_2), 1192 (SO_2 symmetric), and 865 and 819 (substituted aromatic).

References

Baker, B. R. (1975) *Design of Active-Site-Directed Irreversible Enzyme Inhibitors*, Krieger, Huntington, WV.

Berends, F., Rörsch, A., & Stevens, W. F. (1967) in *Proceedings of the Conference on Structure and Reactions of DFP Sensitive Enzymes* (Heilbronn, E., Ed.) p 45, Försvarets Forskningsanstalt, Stockholm.

Berliner, L. J. (1974) *Prog. Bioorg. Chem. 3*, 1.

Berliner, L. J. (1978) *Methods Enzymol. 49G*, 418.

Berliner, L. J., & Wong, S. S. (1974) *J. Biol. Chem. 249*, 1668.

Blow, D. M. (1974) *Isr. J. Chem. 12*, 483.

British Patent (1956) 819 664.

Bruno, G. V. (1973) Ph.D. Thesis, Cornell University.

Buchachenko, A. L., & Wasserman, A. M. (1982) *Pure Appl. Chem. 54* (2), 507.

Buchachenko, A. L., Wasserman, A. M., Aleksandrova, T. L., & Kovarskii, A. L. (1980) in *Molecular Motion in Polymers by ESR* (Boyer, R. F., & Keinath, S. E., Eds.) p 33, Harwood, Chur, Switzerland.

Bullock, A. (1980) in *Molecular Motion in Polymers by ESR* (Boyer, R. F., & Keinath, S. E., Eds.) p 115, Harwood, Chur, Switzerland.

Cardinaud, R., & Baker, B. R. (1970) *J. Med. Chem. 13*, 467.

Carrington, A., & McLachlan, A. D. (1967) *Introduction to Magnetic Resonance*, Harper and Row, New York.

Chignell, C. F. (1979) in *Spin Labeling II. Theory and Applications* (Berliner, L. J., Ed.) p 223, Academic Press, New York.

Fahrney, D. E., & Gold, A. M. (1963) *J. Am. Chem. Soc. 85*, 997.

Freed, J. H. (1972) in *Electron Spin Relaxation in Liquids* (Muus, L. T., & Atkins, P. W., Eds.) p 165, Plenum Press, New York.

Freed, J. H. (1976) in *Spin Labeling. Theory and Applications* (Berliner, L. J., Ed.) p 53, Academic Press, New York.

Freed, J. H., Bruno, G. V., & Polnaszek, C. F. (1971) *J. Phys. Chem. 75*, 3385.

Gold, A. M. (1965) *Biochemistry 4*, 897.

Gold, A. M., & Fahrney, D. E. (1964) *Biochemistry 3*, 783.

Griffith, O. H., Cornell, D. W., & McConnell, H. M. (1965) *J. Chem. Phys 43*, 2909.

Griffith, O. H., Dehlinger, P. J., & Van, S. P. (1974) *J. Membr. Biol. 15*, 159.

Hessing, J. G. M. (1983) *Ph.D. Thesis*, University of Leiden.

Hoff, A. J., Oosterbaan, R. A., & Deen, R. (1971) *FEBS Lett. 14*, 17.

Jost, P. C., & Griffith, O. H. (1978) *Methods Enzymol. 49G*, 369.

Kraut, J. (1977) *Annu. Rev. Biochem. 46*, 331.

Kraut, J., Robertus, J. A., Birktoft, J. J., Alden, R. A., Wilcox, P. E., & Powers, J. C. (1971) *Cold Spring Harbor Symp. Quant. Biol. 36*, 117.

Krinitskaya, L. A. Rozantsev, E. G., & Neiman, M. B. (1966) *Z. Org. Khim. 2* (7), 1301.

Libertini, L. J., & Griffith, O. H. (1970) *J. Chem. Phys. 53*, 1359.

Mehlkopf, A. F. (1970) Internal Report, Department of Applied Physics, University of Technology, Delft.

Mehlkopf, A. F., Smidt, J., & Tiggelman, T. A. (1972) *Rev. Sci. Instrum. 43*, 693.

Morrisett, J. D. (1976) in *Spin Labeling. Theory and Applications* (Berliner, L. J., Ed.) p 273, Academic Press, New York.

Owen, N. L. (1974) in *Internal Rotation in Molecules* (Orville-Thomas, W. J., Ed.) p 157, Wiley, London.

Piette, L. H., & Hsia, J. C. (1979) in *Spin Labelling II. Theory and Applications* (Berliner, L. J., Ed.) p 247, Academic Press, New York.

Polnaszek, C. (1976) Ph.D. Thesis, Cornell University.

Robertus, J. D., Alden, R. A., Birktoft, J. J., Kraut, J. Powers, J. C., & Wilcox, P. E. (1972) *Biochemistry 11*, 2439.

Rörsch, A., Berends, F., Bartlema, H. C., & Stevens, W. F. (1971) *Proc. K. Ned. Akad. Wet., Ser. C 74*, 132.

Rozantsev, E. G. (1970) *Free Nitroxyl Radicals*, Plenum Press, New York.

Sigler, P. B., Jeffrey, B. A., Matthews, B. W., & Blow, D. M. (1966) *J. Mol. Biol. 15*, 175.

Smith, I. C. P. (1972) in *Biological Applications of Electron Spin Resonance* (Swartz, H., Bolton, J. R., & Borg, D., Eds.) p 483, Wiley, New York.

Stevens, W. F. (1969) Ph.D. Thesis, University of Leiden.

Van der Drift, A. C. M. (1983) Ph.D. Thesis, University of Utrecht.

Wong, S. S., Quiggle, K., Triplet, C., & Berliner, L. J. (1974) *J. Biol. Chem. 249*, 1678.

Wright, C. S., Alden, R. A., & Kraut, J. (1969) *Nature (London) 221*, 235.